



THE UNIVERSITY *of* EDINBURGH

Edinburgh Research Explorer

Lowering the excitation threshold of a random laser using the dynamic scattering states of an organosiloxane smectic A liquid crystal

Citation for published version:

Morris, SM, Gardiner, DJ, Qasim, MM, Hands, PJW, Wilkinson, TD & Coles, HJ 2012, 'Lowering the excitation threshold of a random laser using the dynamic scattering states of an organosiloxane smectic A liquid crystal' *Journal of Applied Physics*, vol 111, no. 3, 033106, pp. -. DOI: 10.1063/1.3681898

Digital Object Identifier (DOI):

[10.1063/1.3681898](https://doi.org/10.1063/1.3681898)

Link:

[Link to publication record in Edinburgh Research Explorer](#)

Document Version:

Publisher's PDF, also known as Version of record

Published In:

Journal of Applied Physics

Publisher Rights Statement:

Publisher's Version/PDF: author can archive publisher's version/PDF

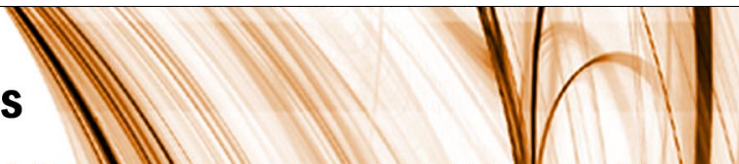
General rights

Copyright for the publications made accessible via the Edinburgh Research Explorer is retained by the author(s) and / or other copyright owners and it is a condition of accessing these publications that users recognise and abide by the legal requirements associated with these rights.

Take down policy

The University of Edinburgh has made every reasonable effort to ensure that Edinburgh Research Explorer content complies with UK legislation. If you believe that the public display of this file breaches copyright please contact openaccess@ed.ac.uk providing details, and we will remove access to the work immediately and investigate your claim.





Lowering the excitation threshold of a random laser using the dynamic scattering states of an organosiloxane smectic A liquid crystal

Stephen M. Morris, Damian J. Gardiner, Malik M. Qasim, Philip J. W. Hands, Timothy D. Wilkinson et al.

Citation: *J. Appl. Phys.* **111**, 033106 (2012); doi: 10.1063/1.3681898

View online: <http://dx.doi.org/10.1063/1.3681898>

View Table of Contents: <http://jap.aip.org/resource/1/JAPIAU/v111/i3>

Published by the [American Institute of Physics](#).

Related Articles

Electro-optical response of the combination of two twisted nematic liquid crystal cells in series and the applicability of the extended Jones matrix

[AIP Advances 1, 042167 \(2011\)](#)

Effect of gold nano-particles on switch-on voltage and relaxation frequency of nematic liquid crystal cell

[AIP Advances 1, 042162 \(2011\)](#)

Single walled carbon nano-tube, ferroelectric liquid crystal composites: Excellent diffractive tool

[Appl. Phys. Lett. 99, 201106 \(2011\)](#)

Liquid crystal bubbles forming a tunable micro-lenses array

[J. Appl. Phys. 110, 074902 \(2011\)](#)

Fluorescence enhancement of dye-doped liquid crystal by dye-induced alignment effect

[J. Appl. Phys. 110, 063532 \(2011\)](#)

Additional information on J. Appl. Phys.


Journal Homepage: <http://jap.aip.org/>

Journal Information: http://jap.aip.org/about/about_the_journal

Top downloads: http://jap.aip.org/features/most_downloaded

Information for Authors: <http://jap.aip.org/authors>

ADVERTISEMENT

	Working @ low temperatures? Contact Janis for Cryogenic Research Equipment Click here to browse our site at www.janis.com	
---	---	---

Lowering the excitation threshold of a random laser using the dynamic scattering states of an organosiloxane smectic A liquid crystal

Stephen M. Morris,^{a)} Damian J. Gardiner, Malik M. Qasim, Philip J. W. Hands, Timothy D. Wilkinson, and Harry J. Coles^{b)}

Centre of Molecular Materials for Photonics and Electronics, Electrical Engineering Division, Department of Engineering, University of Cambridge, 9 JJ Thomson Avenue, Cambridge, CB3 0FA, United Kingdom

(Received 8 November 2011; accepted 1 January 2012; published online 10 February 2012)

Smectic A liquid crystals, based upon molecular structures that consist of combined siloxane and mesogenic moieties, exhibit strong multiple scattering of light with and without the presence of an electric field. This paper demonstrates that when one adds a laser dye to these compounds it is possible to observe random laser emission under optical excitation, and that the output can be varied depending upon the scattering state that is induced by the electric field. Results are presented to show that the excitation threshold of a dynamic scattering state, consisting of chaotic motion due to electro-hydrodynamic instabilities, exhibits lower lasing excitation thresholds than the scattering states that exist in the absence of an applied electric field. However, the lowest threshold is observed for a dynamic scattering state that does not have the largest scattering strength but which occurs when there is optimization of the combined light absorption and scattering properties. © 2012 American Institute of Physics. [doi:10.1063/1.3681898]

I. INTRODUCTION

Random lasers, which rely upon multiple scattering as the feedback mechanism, have attracted considerable attention over the past decade or so because of their remarkable properties such as omni-directional and relatively narrow-band laser emission.¹ Because the only requirements are that the host medium be turbid and a gain medium be present, research has shown that this type of laser action can be observed in a range of scattering media such as laser and semiconductor powders,² nanocrystals,³ and even biological tissues.⁴ Not only is the physics underpinning these lasers rich, but they have great technological potential. To date, a range of applications have been proposed, including friend-or-foe identification, counterfeiting, and display devices.¹

Liquid crystals (LCs) are another form of media that can strongly scatter light, due to high optical anisotropy and order at the molecular level but some disorder at the macroscopic level. Therefore, a number of reports have demonstrated random laser emission in LC media ranging from polymer dispersed LCs with nano-⁵ and micro-scale⁶ droplets to cholesterics in polymer solutions.⁷ The most extensively studied LC phase for random lasers, however, is the nematic phase.^{8–13} In random lasers, an important parameter is the transport mean free path l , which is defined as the distance a photon travels before its direction is randomized, because it influences the excitation threshold for laser emission. This property, which is also inversely proportional to the scattering cross-section, is sensitive to external fields in nematic LCs. Consequently, reports have typically focused on thermally,^{8–10} optically,¹² and electrically¹³ driven

changes in the scattering properties and the subsequent effect they have on the laser characteristics. There have also been studies carried out on the statistical properties of the emission from dye-doped nematic random lasers.¹¹

One key benefit of using LCs in the development of random lasers is their response to electric fields. It is well known that when a nematic LC with a negative dielectric anisotropy is subjected to a low frequency applied electric field, it is possible to induce different scattering states from an otherwise transparent state due to the competition between the restoring dielectric torque and a torque associated with the conductivity anisotropy.¹⁴ As a result, the magnitude of l can be controlled directly by the amplitude of the applied electric field as the sample passes through different scattering states. This has been verified experimentally by Carbone *et al.* using a coherent backscattering technique: it was found that dynamic scattering states of a nematic LC, in the presence of an external electric field, exhibited a particularly low value of l .¹⁵ The dependence of l upon external applied field separates LCs from most other forms of random media for which the scattering configuration is predefined and cannot be readily altered *in situ*.

Smectic A LCs also exhibit light scattering states; however, unlike with nematic LCs, it is possible for the strong multiple scattering states to remain once the applied electric field is removed.^{16–18} Organosiloxane LCs have been shown to be particularly effective materials in which scattering can be readily induced by electrical means at relatively low voltages.^{17,18} A range of intermediate scattering states can be generated and stored indefinitely with different values for l . After doping the material with a laser dye, we have recorded the laser emission characteristics from different states in order to show that the direct control of the scattering strength, and consequently l , results in changes in the excitation threshold energy for such random lasing. Furthermore, it

^{a)}Author to whom correspondence should be addressed. Electronic mail: smm56@cam.ac.uk.

^{b)}Electronic mail: hjc37@cam.ac.uk.

is possible to compare directly the emission characteristics for both static and dynamic (in which the local director is in a constant state of flux) regimes. The results show that this latter regime exhibits the lowest excitation threshold for lasing.

II. SAMPLE PREPARATION

The dye-doped smectic A sample used in this study consisted of siloxane monomesogenic material, referred to herein as 8/2 siloxane (see Fig. 1) and synthesized in-house, with 8 being the length of the alkyl chain attached to a 4-(ω -alkyloxy)-4-cyanobiphenyl mesogenic unit and 2 representing the number of silicon atoms in the pentamethyldisiloxane terminal chain. The organosiloxane compounds exhibit a significantly larger conductivity anisotropy than conventional smectic A compounds and thus are well suited for electric field induced scattering devices.¹⁷ In order to increase the temperature range, the siloxane monomesogen was doped into the wide temperature range nematogen mixture BL006 (Merck KGaA) at a concentration ratio by weight of 40:60. The combination of the organosiloxane monomesogen and the nematogen mixture enhances the temperature range of the smectic A phase (I (78 °C) N (74 °C) S_A (< -50 °C) Kr), increases the birefringence, and reduces the operating voltage.¹⁸ This mixture was then doped with 0.1 wt. % cetyltrimethylammonium bromide in order to ensure that there was sufficient conductivity present to induce the scattering states. The gain medium that was chosen was the laser dye pyrromethene 597 (Exciton), as this has been shown to exhibit a large quantum efficiency in LC hosts.¹⁹ The resultant mixture was capillary filled into a 10 micron thick cell that consisted of indium-tin oxide electrodes and anti-parallel rubbed polyimide surface alignment layers.

III. EXPERIMENTAL PROCEDURES

In order to induce the different scattering states, a bipolar square wave electric field was applied across the sample using a combination of a signal generator (TG1304, Thurlby Thandar) and a high voltage amplifier (built in-house). In all cases, the amplitude of the applied electric field was $E = 12 \text{ V}/\mu\text{m}$. Polarizing optical microscope images of the different sample textures were recorded between crossed polarizers on a BH-2 Olympus microscope using a CCD (Pixelink) camera that was mounted in the photo-tube. To record the dependence of the transmission through the sample as a function of the applied frequency, a photodiode was mounted in the photo-tube in place of the

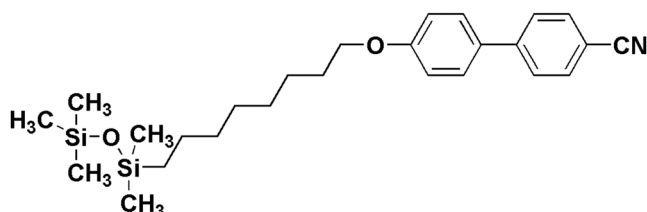


FIG. 1. Chemical structure of the siloxane monomesogen liquid crystal used in this study.

camera, and the output was connected to a digitizing oscilloscope (HP54503 A, Hewlett Packard).

The emission characteristics of the dye-doped smectic A sample were obtained by means of optically exciting the sample with 5 ns pulses at a wavelength of 532 nm, an excitation rate of 1 Hz, and a pump spot size of $\approx 100 \mu\text{m}$ (the source was a Nd:YAG laser, Polaris II, New Wave Research). A high-resolution (0.3 nm) universal serial bus-based spectrometer (HR2000, Ocean Optics) was used to capture the emission from the sample following a series of collection optics. All measurements were carried out at a temperature of 25 °C.

IV. RESULTS AND DISCUSSION

Figure 2 shows experimental results of the normalized transmission of white light through the sample as a function of the frequency of the applied electric field. These measurements, which were reversible, highlight the facile control of the scattering properties and, therefore, the transport mean free path. At low frequencies ($f < 50 \text{ Hz}$), only a very small amount of light is transmitted, as the sample scatters almost all the incident light; at these low frequencies, l is at a minimum. As the frequency is increased above $f = 50 \text{ Hz}$, more light is transmitted as the scattering strength of the sample decreases (l increases), and this continues until the sample is transformed to a transparent state. In this case, the majority of the incident light is transmitted at frequencies above $f = 200 \text{ Hz}$ (the transmission does not reach a value of $T = 1$ due to absorption of the dye). For these high frequencies, the scattering strength reaches a minimum corresponding to a maximum in l .

The change in the alignment of the smectic A for different applied electric field frequencies is illustrated schematically in Fig. 3. Assuming that the sample is initially in the homeotropic state [Fig. 3(a)], if a low frequency ($f < 150 \text{ Hz}$) is applied, a scattering texture forms and evolves as a result of the turbulent motion of the ionic species, due to the competition of the conductivity and dielectric torques. Figure 3(b) depicts the random alignment of the LC, along with a polarizing microscope image of this dynamic

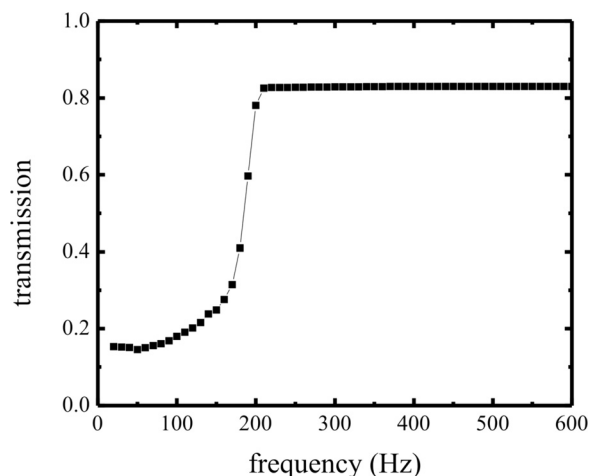


FIG. 2. The transmission of white light through the dye-doped smectic A sample as a function of the frequency of a bipolar electric field at a fixed amplitude of $12 \text{ V}/\mu\text{m}$ and a temperature of 25 °C.

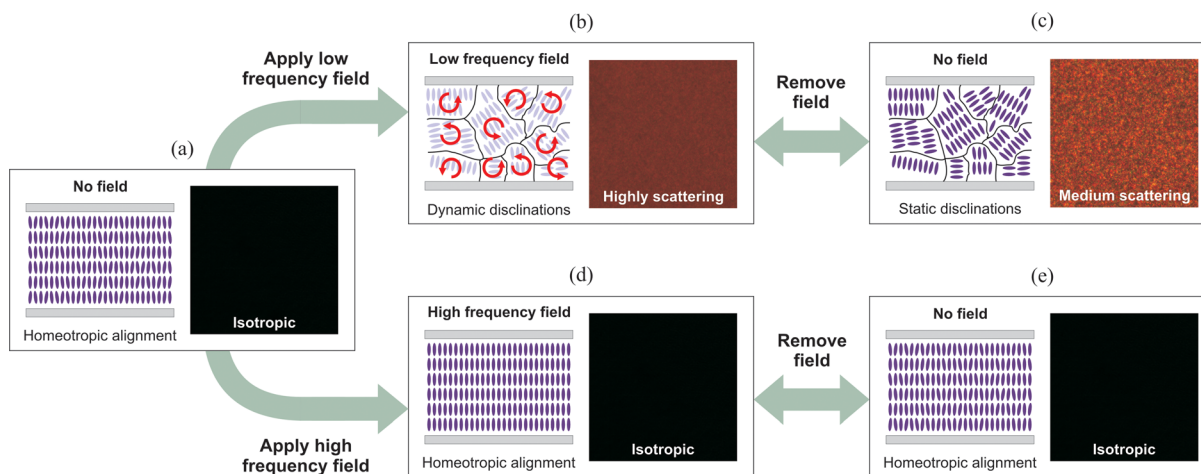


FIG. 3. (Color online) Schematic of the alignment and corresponding polarizing optical microscope images of (a) the initial, pre-field, homeotropic state; (b) the dynamic scattering state that is formed using a frequency $f \approx 100$ Hz; (c) the scattering state after removal of the applied electric field; (d) the homeotropic (transparent) state when subjected to an electric field with a frequency $f > 250$ Hz; and (e) the homeotropic state after the removal of the applied electric field.

scattering state. Once the field is removed, a focal conic (scattering) texture with feature sizes on the order of a few microns is observed, but the turbulent motion is no longer present [Fig. 3(c)]. It is noted that the scattering texture appears to be less opaque in the static case than that observed when the electric field is applied. If, instead, a frequency above $f = 250$ Hz is applied, then the sample remains transparent, as the molecules respond dielectrically to co-align with the direction of the applied electric field. An illustration of the alignment of the LC and a polarizing optical microscope image verifying that the alignment is homeotropic are shown in Fig. 3(d). When the electric field is removed, this homeotropic (transparent) state is retained [Fig. 3(e)].

Additional polarizing optical micrographs of the sample texture with and without an applied electric field are shown in Fig. 4 to highlight the different textures that are formed. These images represent the states of the sample for three different frequencies of applied electric field and the remaining state once the field is removed. Figures 4(a) and 4(b) show the optical texture for a frequency of $f = 20$ Hz and the static

state after removal of the applied field, respectively. The dynamic scattering state that is observed with the field applied is found to decrease in opacity as the frequency is increased; this can be seen in Fig. 4(c) for an applied frequency $f \approx 180$ Hz (corresponding to a point midway up the response curve of Fig. 2). Between $f = 10$ Hz and $f = 150$ Hz, the static scattering states that are formed once the field has been removed appear identical to that shown in Fig. 4(b). However, as shown, the state is quite different for frequencies above $f = 150$ Hz [Fig. 4(d)] and is found to contain both scattering and homeotropic regions. At frequencies above $f = 250$ Hz [Fig. 4(e)], the sample adopts a homeotropic texture as the molecules are forced to align parallel to the applied electric field, as dielectric coupling dominates. From these collective images, it is clear that the smectic A sample can adopt a range of different optical states, each with a different scattering strength and, consequently, a different value of l .

Although there appears to be a large number of different alignments, this study will focus on three distinct states: a

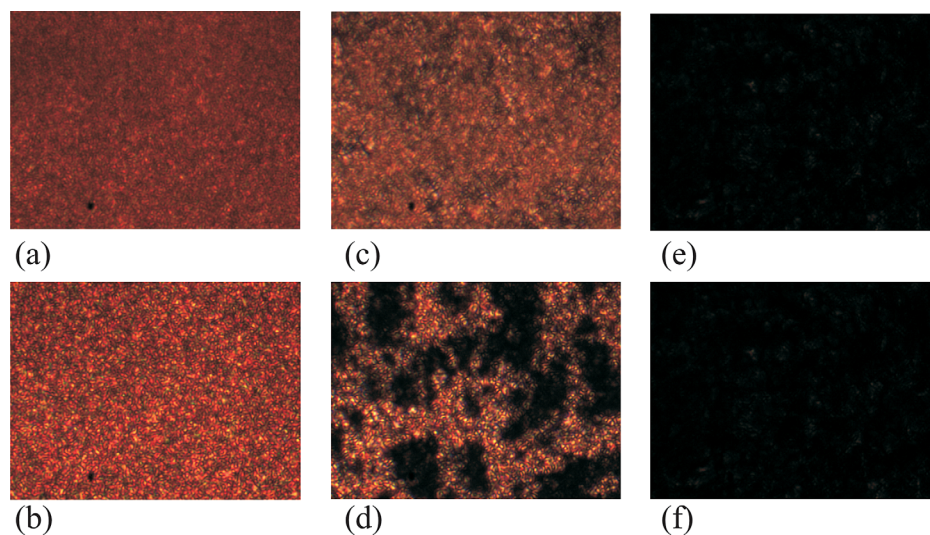


FIG. 4. (Color online) Photographs of the optical texture recorded via a polarizing optical microscope with and without an applied electric field for different applied frequencies at an amplitude of $12 \text{ V}/\mu\text{m}$: (a) $f = 20$ Hz, (b) field removed, (c) $f = 180$ Hz, (d) field removed, (e) $f = 250$ Hz, and (f) field removed. The images are approximately $200 \mu\text{m} \times 300 \mu\text{m}$.

transparent state obtained using frequencies above $f = 250$ Hz, a static scattering state that is generated with frequencies $f \leq 100$ Hz and is formed after the field is removed, and finally a dynamic scattering state that is obtained by maintaining the applied electric field at frequencies $f \leq 100$ Hz. Each state possesses a different value of l , and this is probed indirectly by considering the emission characteristics of each of these states.

The emission spectra of the sample for the three different configurations (transparent state, scattering state, and dynamic scattering state) at the same excitation energy are shown in Fig. 5. For the transparent state [Fig. 5(a)], no discernible emission from the sample was recorded; the sharp spike at 532 nm corresponds to the excitation wavelength, which is more apparent for this configuration, as a greater proportion of the pump beam is transmitted. At the same excitation energy, random laser emission was observed for the static scattering state [Fig. 5(b)]. This is in contrast to a previous study on a smectic A laser that required an electric field to be applied continually in order for random laser emission to be observed.²⁰ Here, the spectrum resembles that of non-resonant random lasing, in which the output consists of a smooth emission profile due to the overlap of neighboring modes, and there is no clear evidence of the narrow linewidth peaks that are typically associated with localized modes.¹ Gain narrowing occurs around the gain maximum ($\lambda \approx 590$ nm), and it is believed that l is independent of wavelength for the sample, unlike in recent studies on Mie resonance-driven random laser emission.²¹ Although laser emission is observed for the static scattering state, the intensity is evidently enhanced two-fold when the electric field is applied [Fig. 5(c)]. This results in a turbulent (dynamic) scattering state as the ionic species propagate chaotically around the gain region at timescales much less than the excitation rate of the pump laser.

To aid in the quantitative determination of the change in the random laser behavior, Fig. 6 presents plots of the peak emission intensity (a) and the full width at half maximum (FWHM) (b) as a function of the excitation energy for the three different states. For the transparent state, the emission

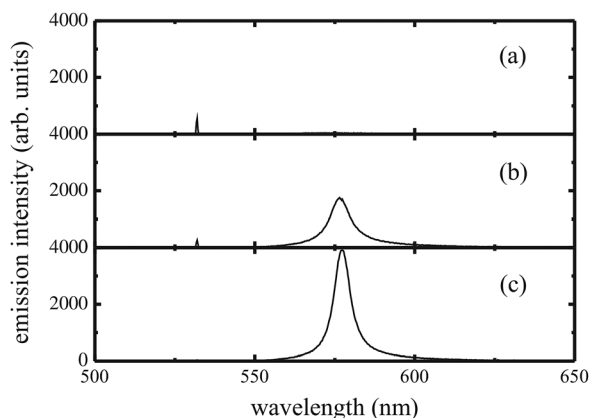


FIG. 5. The emission spectrum from the dye-doped smectic A sample for the three different states ((a) transparent, (b) static scattering, and (c) dynamic scattering) with an excitation energy of $21 \mu\text{J}/\text{pulse}$. The spike at 532 nm marks the pump laser line.

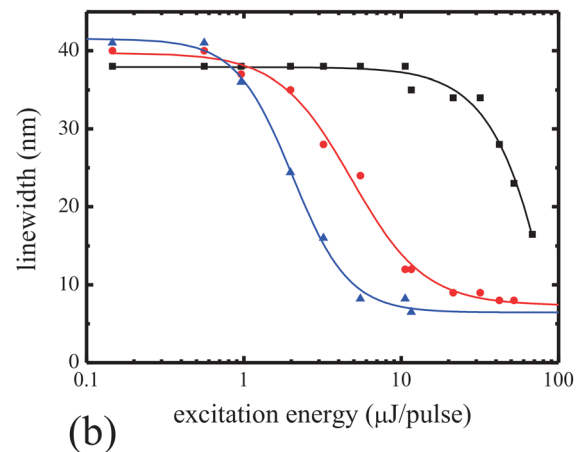
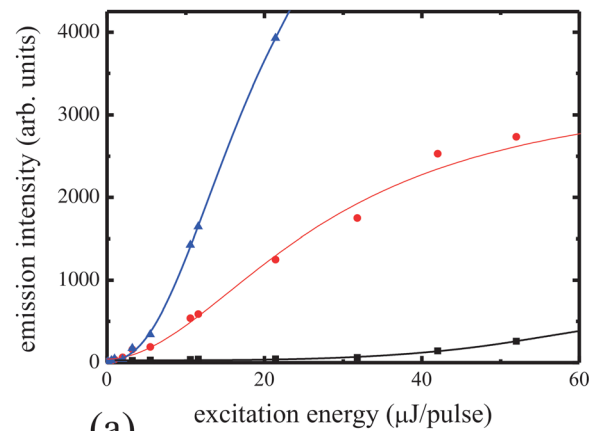


FIG. 6. (Color online) Emission characteristics of the dye-doped smectic A sample for the three different states: transparent (squares), static scattering (circles), and dynamic scattering (triangles). (a) The peak emission intensity as a function of excitation energy and (b) the full-width at half maximum as a function of excitation energy. The lines in (b) represent sigmoidal fits to the experimental data.

intensity is very low, and for the majority of the input energies used herein the spectrum resembled that of the laser dye in the absence of any amplification. The dependence of the FWHM on the excitation energy, which is fitted by a sigmoidal function in Fig. 6(b), shows that gain narrowing does not occur until excitation energies above $15 \mu\text{J}/\text{pulse}$ are achieved. For random lasers, the excitation threshold is typically defined as the point of inflection of a sigmoidal fit through the data points. In this case, the excitation threshold is found to be $E_{\text{th}} > 38 \mu\text{J}/\text{pulse}$. The static scattering state (i.e., on field removal) exhibits a higher emission intensity for all excitation energies [Fig. 6(a)], and gain narrowing starts at the much lower value of $< 1 \mu\text{J}/\text{pulse}$ [Fig. 6(b)]. The excitation threshold, at $E_{\text{th}} = 5 \mu\text{J}/\text{pulse}$, is found to be an order of magnitude or more lower than that of the transparent state, indicating a substantial drop in the transport mean free path between the two states (because $E_{\text{th}} \propto l$, there is a concomitant decrease in l). The lower excitation threshold of the static scattering state than of the transparent state results from the larger scattering cross-section of the micron sized focal conic domains [Fig. 4(b)]. However, the emission intensity is found to be noticeably higher for the dynamic scattering state and is approximately 3 times greater than

that recorded for the static scattering state. In this case, the excitation threshold occurs at $E_{th} \approx 2.7 \mu\text{J}/\text{pulse}$, and the linewidth collapses further to $\Delta\lambda \approx 5 \text{ nm}$. This shows that when the micron sized features of the static scattering state are combined with turbulent ionic motion, l can be further reduced. These results are in good agreement with the low values of l obtained from coherent backscattering measurements for the dynamic scattering state of a nematic LC.¹⁵

Of the three different alignment conditions of the smectic A LC, clearly the most desirable state for efficient random laser emission is the dynamic scattering state, which is obtained by maintaining a low frequency electric field across the sample, because this state has the lowest excitation threshold and the highest slope efficiency (see Figure 6). The question then arises of what might be the optimum applied field frequency for a given applied field. As can be seen from Fig. 7, for the dynamic scattering state, the output is dependent upon the actual frequency that is applied and is not identical for all frequencies in the dynamic scattering regime. From Fig. 2, the minimum transmission is observed for frequencies on the order of $f=50 \text{ Hz}$ or less. However, the optimum value of the frequency for a given fixed electric field amplitude appears to be higher. It can be seen that the random laser output increases with frequency above $f=10 \text{ Hz}$ until it reaches a maximum at $f \approx 100 \text{ Hz}$ before decreasing, with a further increase in the frequency of the bipolar square wave, as the sample approaches the field induced transparent state. Comparison of the excitation energy dependence of the output laser intensity for the different scattering states shows that the intensity is greatest at $f=100 \text{ Hz}$ [Fig. 7(b)]. Threshold energy data confirm the improvement in the performance: the excitation threshold is decreased by $\sim 40\%$ when the frequency of the applied field is changed from $f=10 \text{ Hz}$ to $f=100 \text{ Hz}$, and the linewidth becomes much narrower at lower input pulse energies [Fig. 7(c)].

In order to understand these results, we consider the excitation threshold of a random laser, which can be expressed in terms of the scattering strength σ_s ($\sigma_s \propto 1/l$) and the pump efficiency η_p . The excitation threshold can be written as

$$E_{th} \propto \frac{1}{\sigma_s \eta_p}. \quad (1)$$

From the results presented in Figs. 2–4, it is reasonable to assume that σ_s is smaller at $f=100 \text{ Hz}$ than at lower frequencies, and it is believed that this optimum frequency corresponds to a condition in which the product of the scattering and absorption properties is maximized in accordance with Eq. (1). At low frequencies, scattering is very intense, but very little pump light is able to penetrate the sample, resulting in low absorption of the dye and thus a low η_p . At high frequencies ($f > 100 \text{ Hz}$), there is greater absorption of the dye (i.e., high η_p) but low scattering (low σ_s). At intermediate frequencies, however, both scattering and absorption of the dye are sufficient, and therefore a state exists in which this combination $\sigma_s \eta_p$ is optimized and, thus, E_{th} is minimized.

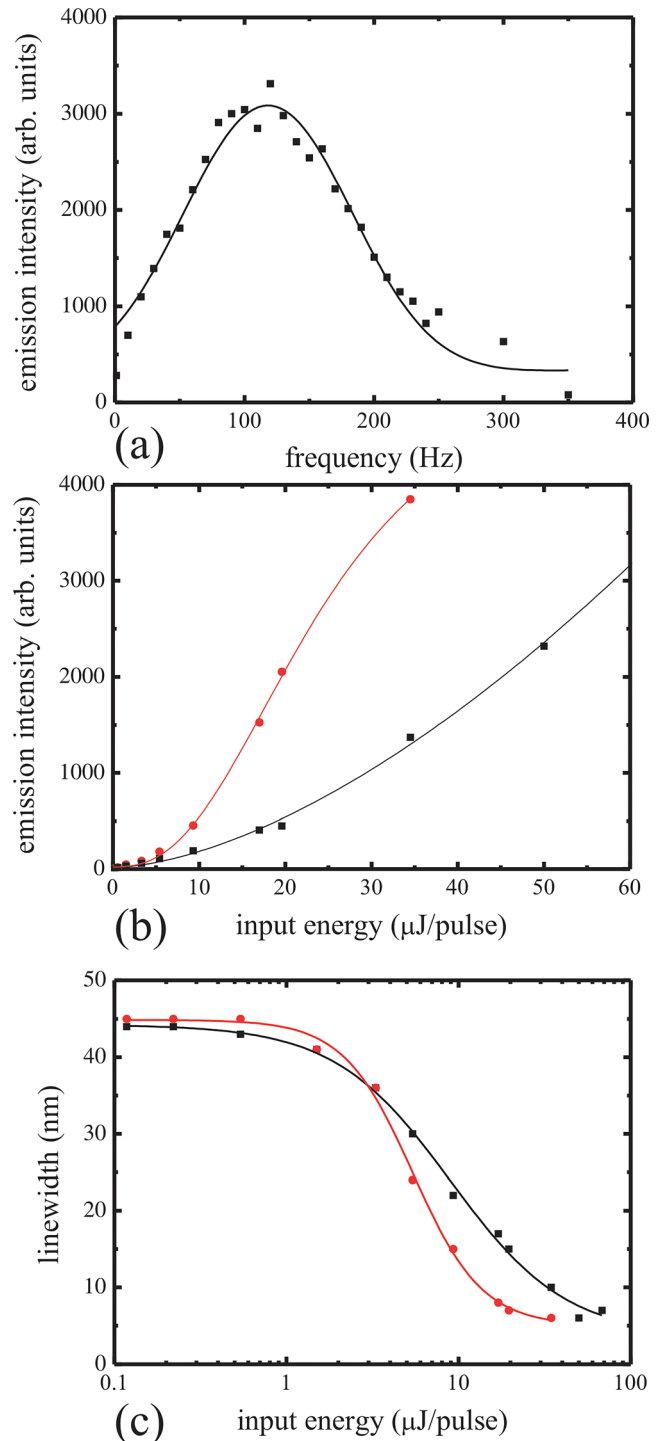


FIG. 7. (Color online) The emission characteristics for different frequencies of the applied electric field. (a) The dependence of the emission intensity as a function of applied frequency. Emission intensity (b) and FWHM (c) as a function of input energy for $f=10 \text{ Hz}$ (squares) and $f=100 \text{ Hz}$ (circles). The lines in (b) are guides for the eye, whereas in (c) the lines represent sigmoidal fits to the experimental data.

V. CONCLUDING REMARKS

Results have been presented on random laser emission from the transparent and scattering states of a multistable smectic A liquid crystal. It is found that the transport mean free path can be reduced by an order of magnitude by simply adjusting the frequency of the applied electric field for a fixed

amplitude. This manifests in a concomitant decrease in the excitation threshold required to initiate laser action. Both transparent and static scattering states are stable in zero-field, but the lowest excitation threshold is observed when electrohydrodynamic instabilities are present, which enhance the scattering properties by adding field-induced fluctuations of the local refractive indices to the scattering features of the focal conic texture. The use of such dynamic scattering states might thus play an important role in achieving very low excitation thresholds in liquid crystal random lasers.

ACKNOWLEDGMENTS

The authors gratefully acknowledge the Engineering and Physical Sciences Research Council for financial support through Coherent Optical Sources based upon Micromolecular Ordered Structures (COSMOS) Technology Translation Grant No. EP/H046658/1. One of the authors (SMM) gratefully acknowledges The Royal Society for funding.

¹See, for example, D. S. Wiersma, *Nat. Phys.* **4**, 359 (2008).

²H. Cao, Y. G. Zhao, S. T. Ho, E. W. Seelig, Q. H. Wang, and R. P. H. Chang, *Phys. Rev. Lett.* **82**, 2278 (1999).

³J. Fallert, R. J. B. Dietz, M. Hauser, F. Stelzl, C. Klingshirn, and H. Kalt, *J. Lumin.* **129**, 1685 (2009).

⁴R. C. Polson and Z. V. Vardeny, *Appl. Phys. Lett.* **85**, 1289 (2004).

⁵Y. J. Liu, X. W. Sun, H. I. Elim, and W. Ji, *Appl. Phys. Lett.* **89**, 011111 (2004).

⁶S. Gottardo, S. Cavalieri, O. Yaroshchuk, and D. S. Wiersma, *Phys. Rev. Lett.* **93**, 263901 (2004).

⁷B. He, Q. Liao, and Y. Huang, *Opt. Mater.* **31**, 375 (2008).

⁸D. Wiersma and S. Cavalieri, *Nature (London)* **414**, 708 (2001).

⁹S. Ferjani, V. Barna, A. De Luca, C. Versace, N. Scaramuzza, R. Bartolino, and G. Strangi, *Appl. Phys. Lett.* **89**, 121109 (2006).

¹⁰G. Strangi, S. Ferjani, V. Barna, A. De Luca, C. Versace, N. Scaramuzza, and R. Bartolino, *Opt. Express* **14**, 7737 (2006).

¹¹S. Ferjani, L. Sorriso-Valvo, A. De Luca, V. Barna, R. De Marco, and G. Strangi, *Phys. Rev. E* **78**, 011707 (2008).

¹²C.-R. Lee, J.-D. Lin, B.-Y. Huang, T.-S. Mo, and S.-Y. Huang, *Opt. Express* **18**, 25896 (2010).

¹³C.-R. Lee, J.-D. Lin, B.-Y. Huang, S.-H. Lin, T.-S. Mo, S.-Y. Huang, C. T. Kuo, and H.-C. Yeh, *Opt. Express* **19**, 2391 (2011).

¹⁴B. Bahadur, in *Handbook of Liquid Crystals*, edited by D. Demus, J. Goodby, G. W. Gray, H.-W. Spiess, and V. Vill (Wiley VCH, Berlin, 1997), Vol. 2A, p. 243.

¹⁵F. Carbone, A. De Luca, V. Barna, S. Ferjani, C. Vena, C. Versace, and G. Strangi, *Opt. Express* **17**, 13436 (2009).

¹⁶D. Coates, W. A. Crossland, J. H. Morrissy, and B. Needham, *J. Phys. D: Appl. Phys.* **11**, 2025 (1978).

¹⁷D. J. Gardiner and H. J. Coles, *J. Appl. Phys.* **100**, 124903 (2006).

¹⁸D. J. Gardiner and H. J. Coles, *J. Phys. D: Appl. Phys.* **39**, 4948 (2006).

¹⁹C. Mowatt, S. M. Morris, M. H. Song, T. D. Wilkinson, R. H. Friend, and H. J. Coles, *J. Appl. Phys.* **107**, 043101 (2010).

²⁰S. M. Morris, A. D. Ford, M. N. Pivnenko, and H. J. Coles, *Appl. Phys. Lett.* **86**, 141103 (2005).

²¹S. Gottardo, R. Sapienza, P. D. García, A. Blanco, D. S. Wiersma, and C. López, *Nat. Photon.* **2**, 429 (2008).